STRUCTURE AND INFRASTRUCTURE ENGINEERING
https://doi.org/10.1080/15732479.2020.1850803

Load rating of bridge-size reinforced concrete arch culverts

Akram Jawdhari[a], Abheetha Peiris[b] and Issam Harik[c]

[a]Department of Civil Engineering, Queen's University, Kingston, ON, Canada; [b]Kentucky Transportation Center, University of Kentucky, Lexington, KY, USA; [c]Department of Civil Engineering, University of Kentucky, Lexington, KY, USA

ABSTRACT

Of the 604,485 bridges in the United States, approximately 21% are culverts having a span of 6 m (20 ft) or greater. The load rating of typical bridges presents numerous challenges. Developing load ratings for non-typical structures, such as buried arch-shaped culverts is more complex because of the culverts' unique geometric configuration and their interaction with soil media. This paper proposes an alternative analytical method for load rating in-service reinforced concrete (RC) arch culverts that overcomes the limitations of the widely used elastic frame concept while being straightforward to implement. The proposed analytical method uses two-dimensional finite element models of the arch structure and surrounding soil media. The finite element model was first validated against experimental tests on a full-scale RC arch culvert, subjected to simulated live loads. The validated FE model was used in load rating analysis of 21 RC arch culverts with large fills. It was found that for arch culverts with fills exceeding 2.43 m (8 ft.), the controlling actions are bending moments at the crown and haunch. For culverts with fills greater than 3.05 m (10 ft.), live load effects become negligible. A revised rating formula is proposed for culverts with this characteristic.

ARTICLE HISTORY
Received 16 December 2019
Revised 6 August 2020
Accepted 6 August 2020

KEYWORDS
Arch culverts; bridges; finite element method; live loads; load rating; reinforced concrete

1. Introduction

Bridge collapses in the United States (US) resulting in human loses and property damages (e.g. the I-35W Mississippi River bridge in 2007) have prompted executive and legislative authorities to enact more stringent measures to ensure that in-service bridges operate safely and reliably. As part of these efforts several bridge inspection and maintenance guides have been published, such as the National Bridge Inspection Standards (NBIS), the Federal Highway Administration's (FHWA) *Bridge Inspector's Training Manual 70* (Manual 70), the American Association of State Highway Officials' (AASHO) *Manual for Maintenance Inspection of Bridges*, and the *Culvert Inspection Manual* [Bridge Inspector's Reference Manual, BIRM (2012)]. These guides provide valuable instructions on when and how to inspect and evaluate bridge structures. For example, NBIS requires load ratings for all highway bridges located on public roads; if the rating is insufficient, it should be posted, for all legal loads and un-restricted routine permit loads (NBIS 2014).

As the population has grown over the past 50 years, traffic volumes and truck weights have increased in order to deliver more goods and services. At the same time, aging, environmental exposure, and other natural events deteriorate infrastructure. The combined effects of higher traffic volumes and infrastructure deterioration make the structural evaluation of bridges and culverts of paramount importance. However, the load rating of typical bridges is not simple, and that of non-typical structures, such as buried arch-shaped culverts, is even more complex because of their unique geometric configurations and their interactions with soil media (Seo, Wood, Javid, & Lawson, 2017; Wood, Lawson, Surles, Jayawickrama, & Seo, 2016; Wood et al., 2017).

While many researchers have studied arch culverts (Boothby, Fanning, & Roberts, 2002; Fanning & Boothby 2002; Wu, 2010), a unified structural evaluation strategy is still lacking, perhaps due to these structures' complexity. One of the oldest analytical methods for evaluating masonry arches is the MEXE (Military Engineering Experimental Establishment). This semi-empirical method was developed in the 1940s by the United Kingdom's military during World War II and provides a quick and conservative assessment of bridge capacity under the passage of heavy military vehicles (Chajes, 2002; Halden, 1995; Wu, 2010). Another analytical method, with a sounder theoretical basis that relies on assumptions about kinematical energy, is the *mechanism method*.

This method assumes that under a concentrated force the arch can develop a failure mechanism by four plastic hinges (Bjurstrom & Lasell, 2009; Brencich & Francesco, 2004). The *mechanism method* offers a reasonably good estimate of an arch structure's load capacity under an ultimate limit state (collapse), provided that location of the hinges is predetermined or adequately presumed. However, this method is not designed to evaluate the forces on arches

CONTACT Akram Jawdhari akram.jawdhari@queensu.ca
Supplemental data for this article is available online at https://doi.org/10.1080/15732479.2020.1850803.

subjected to dead or live loads. Currently, powerful computers and reliable finite element tools are widely used to perform two- and three-dimensional finite element analyses of arch structures (Aagard, 2007).

2. Elastic frame analysis

Elastic frame analysis, which is used mainly to evaluate thrust and bending forces in arch structures, has gained popularity due its relative simplicity, the availability of inexpensive structural software to conduct the analysis, and familiarity of such tools among engineers (Mousavi, Jayawickrama, Wood, & Lawson, 2017; Wu, 2010). Early instructions on the elastic frame method were published in the United Kingdom and detailed in the manual for the Assessment of Highway Bridges and Structures (AHBS 1993). In these guides, the buried arch culvert structure is represented by a unit-wide section of the arch, while the arch is divided into at least 10 straight segments to accurately represent its shape. Beam elements with elastic material properties are used within each segment. Boundary conditions, by restricting vertical movement and allowing for rotation and partial horizontal movement, are assumed at the arch's stems (also known as springing). A distribution formula that considers the dissipation of live loads through the soil medium is used to convert vehicular wheel loads to nodal forces at the arch level (Figure 1) (Acharya, 2012; Wood, Lawson, Jayawickrama, & Newhouse, 2015).

Several state departments of transportation (DOTs) in the US have adopted the elastic frame method to prepare load ratings for arch structures (Boothby; Boothby, Domalik, & Elgin, 1997; Boothby & Fanning, 2004; Kim, Garro, & Doty, 2009; Lawson et al., 2017; Wu, 2010). For example, Boothby et al. (1997) submitted a study to the Ohio DOT that used elastic frame analysis to load rate 139 masonry arch bridges and several masonry arch culverts in Ohio. Chajes (2002), under the direction of the Delaware DOT, used the elastic frame approach to load rate 27 reinforced concrete arch bridges in desperate need of structural assessment. The Massachusetts DOT (MassDOT) LRFD Bridge Manual (2013) also relies on the elastic frame analysis to load rate arch structures. In their culvert rating guide prepared for Texas DOT, Lawson et al. (2017) laid out the details of what they referred to as "LEVEL1 ANALYSIS" for load rating reinforced concrete box culverts (RCBCs), using the elastic frame method.

2.1. Limitations of elastic frame analysis

Although the elastic frame analysis provides a quick, simple, and reasonable estimation for the axial and bending forces of an arch structure (Wood et al., 2015), several challenges arise when attempting to use the method. First, it requires additional computational efforts to supplement the frame model. Dead loads from the weight of soil, subgrade, and pavement are calculated using spreadsheets or mathematical packages (Boothby; Chajes, 2002). In some instances, the soil component at the shoulder of the arch is approximated as having a triangular shape to determine its weight, or is omitted in the calculations. Additionally, computational efforts are required to account for the distribution of live loads through soil fill while applying an equivalent set of forces at some locations within the arch frame. For buried structures such as culverts, a well-established practice is to distribute live load over a linearly increasing trapezoidal region, with a slope governed by the ratio between x and y (Figure 1). The live load distribution is more complex than the trapezoidal model, which is considered reasonable and practical. There are several estimates for the slope of the trapezoidal zone. For example, the current AASHTO LRFD design code assumes a slope of 1.15 (x) to 1 (y), (AASHTO, 2017).

Generally, a theoretical formula that contains the presumed (x/y) slope, along with other inputs, is implemented in a mathematical platform and used to determine equivalent nodal or beam forces at some locations within the one-dimensional arch model. For illustration, Figure 1, shows an arch frame exposed to a single wheel load located at some distance to the left of the arch's centerline. Based on the given load position, fill height, arch shape, number of arch segments, and presumed live load distribution slope, equivalent arch frame forces will only be determined at nodes (n) and (n + 1), located at elevations d_n and d_{n+1}, respectively. If any of these inputs change, the location and number of nodes receiving the load, as well as the intensity of the equivalent force, will be different. Second, the soil surrounding the arch provides a resistance when the arch is under dead or live loads. This resistance is called passive soil pressure (Aagard, 2007). To incorporate this soil pressure into the frame model, one must assume a lateral earth pressure or generate soil springs with stiffness constants pertinent to the soil properties (Lawson et al., 2017). For this, the lateral pressure or springs should be applied only to the arch portions that deform into the soil. Locating those portions is challenging, especially for live loads in which the arch's deformation shape changes continuously with the truck position.

Due to the inconvenience, and in some instances difficulties, of accompanying computations of dead and live loads effects and the contribution of soil media surrounding the arch, most of the time approximations are made. For example, Boothby et al. (1997), Boothby, Chajes (2002), and Boothby and Fanning (2004) made the following approximations: (1) the passive soil pressure is neglected, and (2) the truck position causing maximum effects (axial forces, bending moments) in the arch occurs when the rear axle(s) is located either on top of the arch's crown or at quarter span point. In this scenario, only the weight of the rear axle(s) is factored into load rating computations, while the contribution of the front axle(s) is disregarded. Although neglecting passive soil pressure can give acceptable results for arch bridges with low fill heights, neglecting the passive pressure of buried arch culverts with large fills significantly underestimates arch resistance (Aagard, 2007).

The approximation of truck's position causing maximum forces might be admissible for arch bridges with short spans

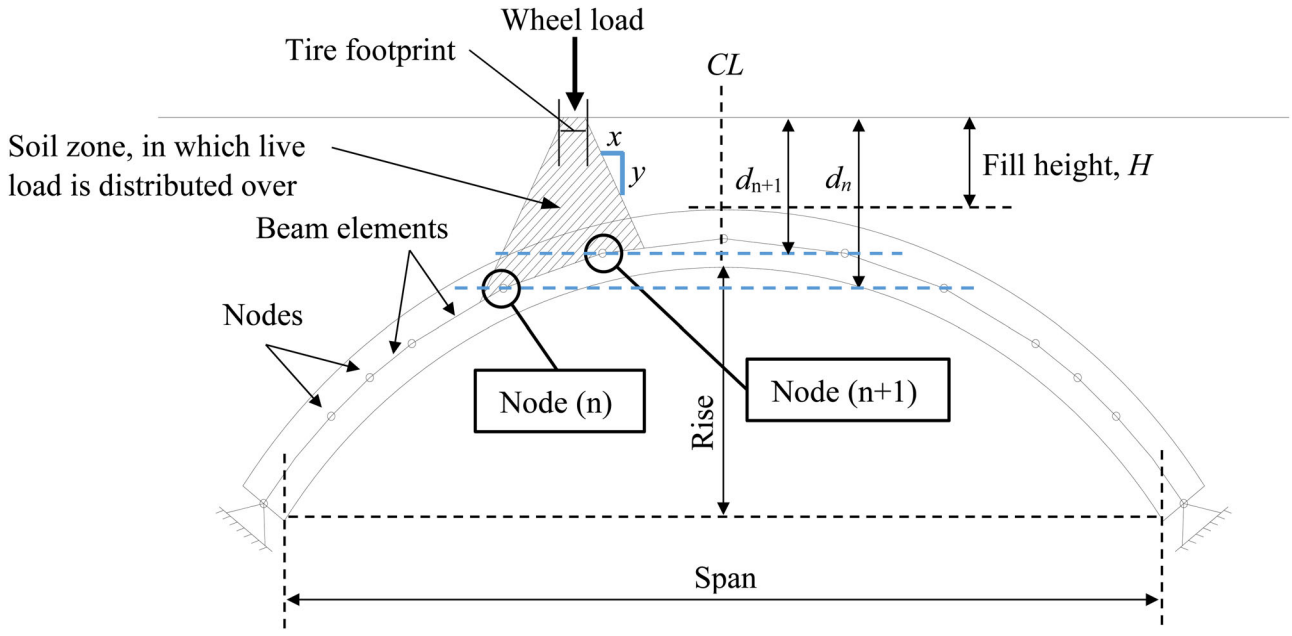

Figure 1. Elastic frame analysis method [after Boothby et al. 2000].

[3–4.6 m (10–15 ft.)] that are traversed by trucks with one or two heavy axles (Gilbert, Melbourne, & Smith, 2006). However, this approximation has not been tested for medium- to long-span arches traversed by trucks with closely spaced multi-axles, such as AASHTO special hauling vehicles (SHVs). According to Sivakumar, Moses, and Ghosn (2007), SHVs produce stresses on highway bridges that exceed the stresses caused by AASHTO standard trucks by 20–50%. Lawson, Seo, Surles, & Morse, 2018 conducted a load rating study on RCBCs using the standard HS-20 truck, SHVs, and HL-93 design tandem live load. Although they found the rating factor from HS-20 truck to dominate for the specific rated box culverts, they concluded that other truck types might be more critical, depending on the culvert geometry, span, axle spacing, and cover soil thickness.

3. Two-dimensional finite element models

The structural response of masonry and concrete arches subjected to live loads can be separated into two parts: the response along the span of the arch (longitudinal effects), and the response in the direction perpendicular to the span (transverse effects) (Chajes, 2002; Fanning, Boothby, & Roberts, 2001). Most of the research on arch structures has focused on the behavior of the arch along the span, and within that context, elastic frame analysis or two-dimensional (2-D) finite element (FE) models are widely used. In rare circumstances, arch failure might initiate by the overturning or sliding of spandrel walls for masonry arches, or formation of longitudinal cracks in the arch barrel for concrete arches due to transverse effects (Chajes, 2002; Fanning et al., 2001; Fanning & Boothby, 2002). In these cases, a three-dimensional FE models or similar methodology must be used to capture the transverse effects (Chajes, 2002).

When the arch structure is subjected to service loads (e.g. weight of the arch, fill, and truck loads), it can be reasonably assumed that the compacted soil fill is within linear elastic range (Aagard, 2007; Katona, Meinhert, Orillac, & Lee, 1979). Using linear elastic property for the backfill material is a valid approximation if the tensile stress induced by the live load is less than the compressive pressure at rest — in other words, no significant tensile stresses form in the backfill (Andersson, 2011). Experimental and numerical research on arch structures loaded with regular service loads has shown that the arch is well under elastic stress range (e.g. no observations of excessive cracks, plastic deformations, or other signs of distress that indicate a plastic behavior) (Boothby et al., 1997; Citto & Woodham, 2014; Fanning et al., 2001). Elastic fill material properties have also been implemented in load rating of RCBCs (Lawson et al., 2017; Wood et al., 2017).

4. Current study

The current study proposes a guideline for load rating RC arch culverts with large fill heights by using 2-D FE models to resolve the limitations of the elastic frame method. The load rating procedure follows the general specifications laid out in AASHTO Manual for Bridge Evaluation (MBE 2015). The load rating was carried out for two rating methods: the Load Factor Rating (LFR) and the Allowable Stress Rating (ASR), at both the Inventory and Operating rating levels. Finite element models were generated in STAAD Pro V8i (2012) to identify the axial forces (thrusts) and bending moments at critical sections along the arch ring. The elastic frame concept was used to model the arch ring. To overcome elastic frame model's limitations, the soil and pavement components were modeled discretely. Plane (quadrilateral and triangular) elements were used to model the soil medium, while the pavement layer and arch ring were modeled using beam elements.

The level of computational effort required to perform discrete modeling of the soil and pavement may be comparable to the level of effort needed to manually calculate dead and live load effects using conventional elastic frame models. The modeling used as part of this study has several advantages and these include: (a) automatic determination of the self-weight of all the model's parts (e.g. soil at shoulder of arch); (b) automatic inclusion of the passive soil pressure due to the Poisson's ratio effects available in the plane elements used to model the soil media; and (c) the *moving load generation* option, available in most current structural software, where the entire truck can be generated and placed at the road level and moved across the length of the model. Consequently, there is no need to use live load distribution formulas or approximate the position of truck that causes maximum forces. Within the 2-D FE model, maximum forces are automatically populated in the post-processing solver, along with the truck's position when it causes those forces. This also enables the inclusion of all truck axles (i.e. rear, front, tandem, and multi-axle) and creates a solution that resembles actual field conditions. Users can also easily modify the model dimensions, element mesh, materials, and live load inputs when necessary.

4.1. Geometrical model

The FE model was constructed with the RC arch ring, soil medium, concrete footing, subgrade base, and pavement, representing a 0.30 m (1 ft.) wide section of a culvert structure. Additional features, such as spandrel walls, head walls, guardrails, and wings, were not included in the 2-D FE model. Those parts cannot be modeled discretely in a 2-D model, but their approximate effects can be added by adjusting the stiffness or the thickness of the arch ring. For load rating purposes, and to provide a simple yet conservative analysis procedure, the model did not account for additional components. The arch ring was divided into 30 straight beam elements located along the centerline of the arch ring. This number of segments -three times the recommended minimum number- was selected based on the authors' judgment, but it does not replace the recommended value. Arches with a varied wall thickness (tapered) were accounted for in the current model by using a stepwise thickness procedure. Each segment was assigned a thickness determined at the center of the segment.

The soil medium was modeled using plane (quadrilateral and triangular) elements, with an average element side length of 0.3 m (1 ft.) based on guidance presented by Lawson et al. (2017). Only a single 2-D element is available in STAAD PRO software. The user can select it to be a membrane only element or a combined membrane and bending element. Due to the 2-D model geometry of the RC arch culvert, a membrane only plane stress element is selected for the soil. The selected mesh size of 0.30 m (1 ft.) is smaller than the mesh used in several other studies (Acharya, 2012; Wood et al., 2017). In STAAD PRO, the automated moving load generation capability is not available for plane elements but is available for beam elements. Consequently, and in order to overcome this limitation, 2 D beam elements are deployed to model the pavement layer. The beam elements, having rotational and translational degrees of freedom (DOF), were laid on the plane elements, having translational DOF, with coinciding node connection. This approximation did not influence the results.

A parametric study was performed to examine the effects of horizontal and vertical soil extensions to the left, right, and beneath the arch on the axial and bending forces of the arch. A typical RC arch culvert, with a span (S) of 9.14 m (30 ft.), a rise (R) of 5.50 m (18 ft.), and an arch thickness of 0.30 m (1 ft.) was modeled and subjected to dead load effects, which consisted of the self-weights of the arch and soil. The fill height (H) was assumed to be 1.22 m (4 ft.); typical material properties (elastic modulus and density) were assigned to the concrete arch and soil. The required discrete soil model length on either side of the arch was investigated first by modeling the soil parts above the arch, and then by varying the horizontal length (L_s) from 0.25-to-3 times the span length [Figure 2(a)].

Figure 2(b) shows the variation of thrust at the springing and bending moments at the crown and haunch (located at quarter span) with respect to the ratio of horizontal soil length to the span (L_s/S). Varying the L_s/S ratio did not significantly influence either the thrust at springing or the bending moment at haunch. On the other hand, the moment at the crown decreased when L_s/S ratio increased, until reaching an approximate L_s/S of 2.0. M_c decreased from 7.15 kN-m at $L_s/S = 0.25$, to 6.02 kN-m at $L_s/S = 1.00$, to 5.27 kN-m at $L_s/S = 2.00$ (7.2% less than M_c at $L_s/S = 1.00$). A ratio of $L_s/S = 1.00$ was selected for the model since it reduces the computational effort and leads to conservative rating factors, when compared with $L_s/S > 1.00$. The effects of vertical soil depth, H_s, below the arch was examined using the FE model with $L_s/S = 1.00$ [Figure 3(a)]. Figure 3(b) shows the variation of thrust at the springing point and bending moments at crown and haunch points with respect to the ratio of vertical soil depth over the span, (H_s/S) . M_c decreased from 8.11 kN-m at $H_s/S = 0.25$, to 6.73 kN-m at $H_s/S = 1.00$, to 6.28 kN-m at $H_s/S = 2.00$ (6.7% less than M_c at $H_s/S = 1.00$). A ratio of $H_s/S = 1.00$ was selected for the model following the same reasoning for the selection of $L_s/S = 1.00$.

After finalizing the 2-D FE model's dimensions, the soil medium was assumed to consist of the following elements, based on typical culvert construction procedures: (1) crushed stone base in the vicinity of the arch, (2) bedrock or undisturbed natural soil beneath the arch, (3) backfill soil, and (4) a layer of subgrade beneath the pavement. The crushed stone part was given the following dimensions: 1.83 m (6 ft.) on the sides of the arch (L_{cst}), 0.30 m (1 ft.) above the arch, (H_{cst}), and 0.30 m (1 ft.) beneath the arch footing (H_{csb}).

Figure 4 displays the geometry of the soil parts and the entire model. All soil parts were modeled as plane elements. The model was supplied with boundary conditions of roller supports along the vertical and bottom edges of the model (Figure 4), following recommendations of Lawson et al.

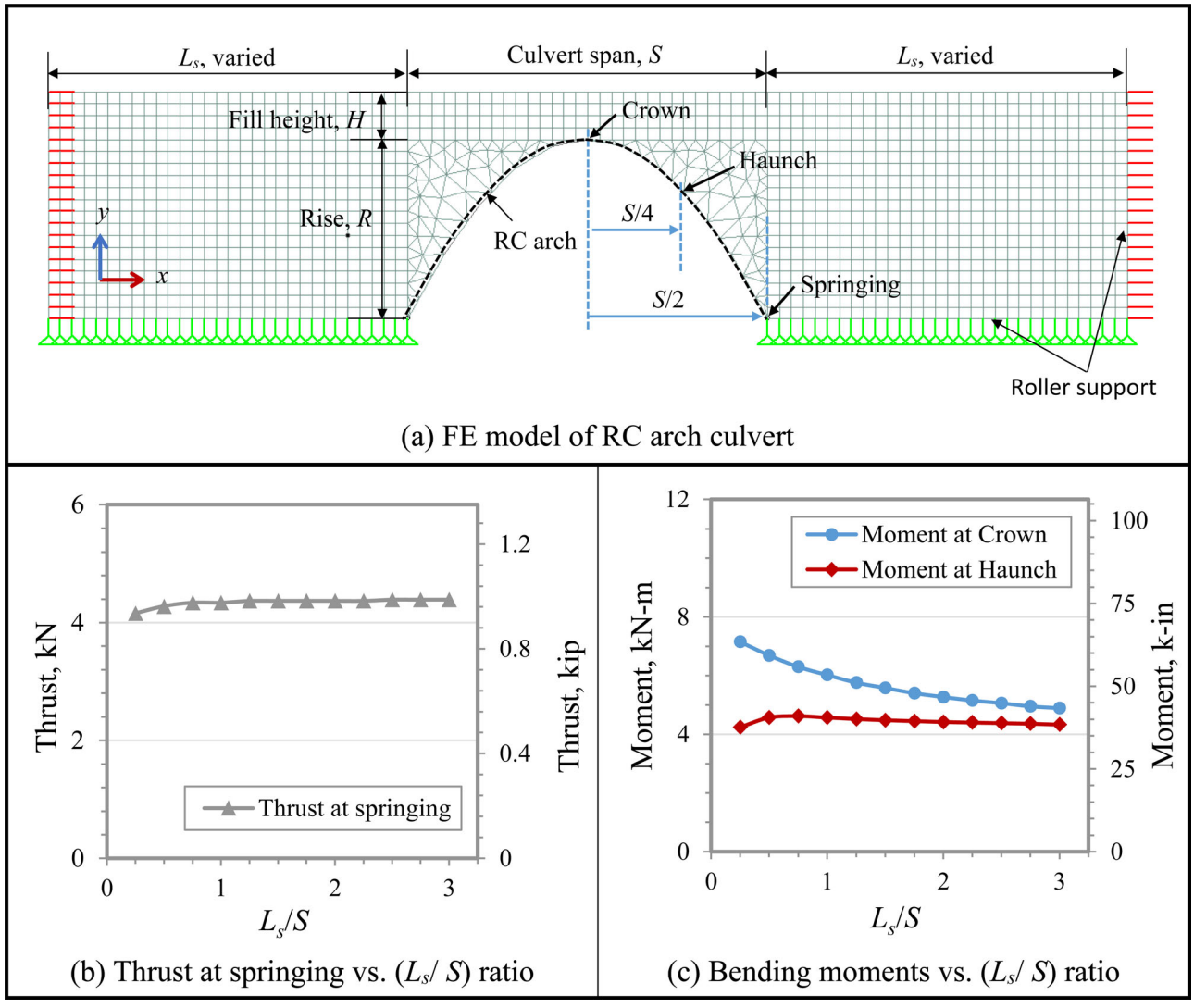

Figure 2. Variation in the magnitude of the thrust and bending moments of an RC arch with respect to horizontal soil length-to-span ratio (L_s/ S).

(2017). Most of the culverts examined in this study had a reinforcement layout consisting of top and bottom layers (which is typical of double-reinforced members) that ran all the way to the footing. However at the same time, the arch was connected to the footing by a shear key. This calls for an arch-footing connection somewhere between moment connection and moment release. A moment release (hinge) connection was selected to provide a simple and conservative rating procedure.

4.2. Material properties

The model assumed an arch constructed of reinforced concrete. If the plans indicated a value for the concrete's compressive strength, f'_c (input for the LFR rating), concrete allowable stress, f_c (input for ASR rating), and the yield strength of the steel reinforcement, f_y (input for the ASR and LFR rating), these numbers were directly used. If there were no data on concrete and steel strengths, suggested values based on construction year were used (sourced from MBE 2015). In the FE model, the concrete elastic modulus, E_c, was the only required input for the elastic analysis of the arch ring. E_c was determined according to the American Concrete Institute [ACI 318-14 (2014)] code. To calculate the arch's sectional capacity and determine the arch's load rating factor, E_c, f'_c, f_c, and f_y were the only data required.

The soil data for culverts considered for load rating in this study are not available in most culvert plans. Typical soil material properties were selected based on the recommendation of Hopkins, Beckham, Sun, and Ni (2001) with supplemental guidance from transportation engineers at the Kentucky Transportation Cabinet (KYTC) (Table 1). Values in Table 1 were identified to provide a simple and conservative load rating analysis in the absence of field test data. It should be noted that the elastic modulus of the soil is dependent upon factors such as the type of soil, moisture content, density etc. As pointed out by Mousavi et al. (2017), a more accurate method of analysis may also be the use of two different soil stiffnesses for dead and live load.

The soil material properties can be revised provided accurate field test data are available. The elastic moduli for the different soil regions around a culvert were conservatively estimated based on Resilient Modulus values for Kentucky Soils (Hopkins et al., 2001). In Table 1, a value of 138 GPa (20

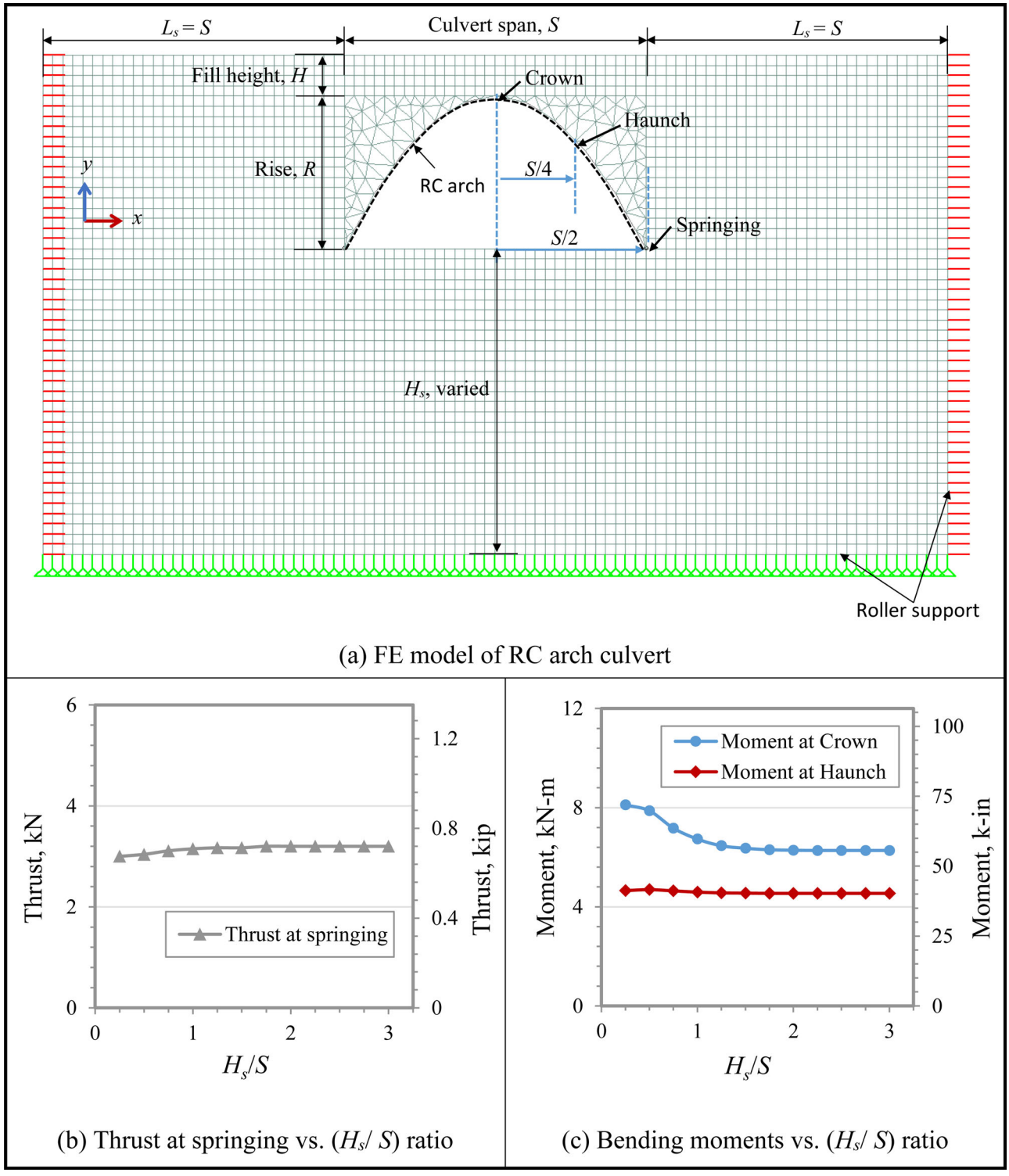

Figure 3. Variation in the magnitude of the thrust and bending moments of an RC arch with respect to vertical soil length-to-span ratio (H_s/ S).

ksi) was chosen for the elastic modulus of compacted backfill. This corresponds to a medium level soil as defined by Lawson et al. (2017). The same stiffness value was also used in (Wood et al., 2017) in load rating RCBCs. The shear modulus, G, is another material property required in the FE formulation of plane elements used in modeling soil parts and concrete footing. Shear modulus was calculated with the following equation, which is applicable for soils under low stresses (Krajcinovic, 1996; Lekhnitskii, 1963):

$$G = \frac{E}{2(1+\nu)} \tag{1}$$

4.3. Loading procedure

The arch culvert was subjected to a set of dead and live loads. The dead loads included the self-weight of the concrete arch and footing, soil parts, and pavement. Live loads

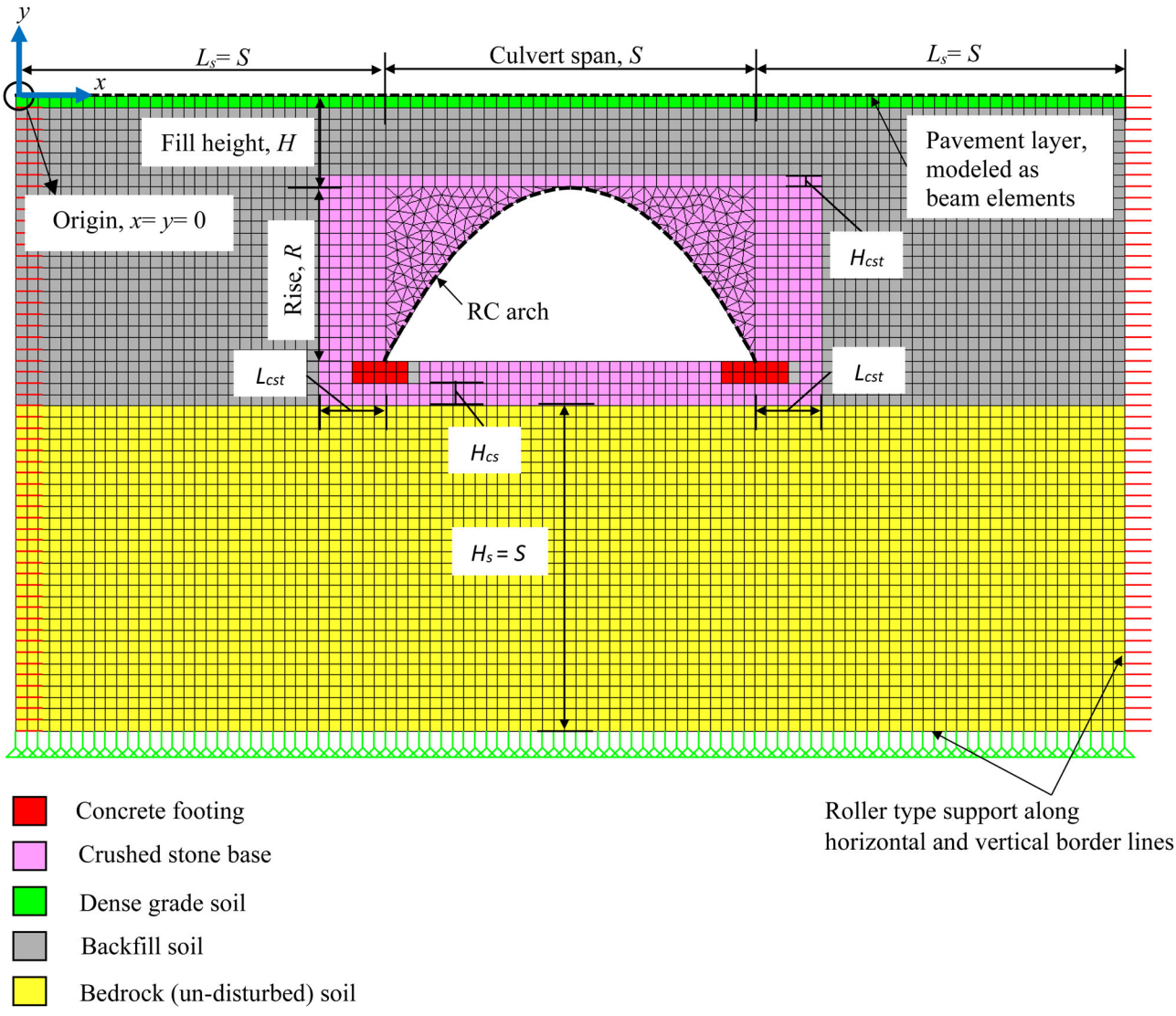

Figure 4. Typical FE model for load rating RC arch culverts.

Table 1. Material properties used in the 2-D FE model and load rating procedure.

Material	Modulus[a] (Mpa)	Poisson's ratio	Density[b] (kg/m3)
Arch and footing concrete[c]	$E_c = 4700\sqrt{f'_c}$	0.20	2400
Pavement concrete[d]	2068	0.20	2400
Subgrade[e]	414	0.35	2162
Compacted backfill[f]	138	0.35	2002
Crushed stone base[g]	278	0.35	2082
Bedrock	6895	0.30	2082

[a]1.0 MPa = 145 psi.
[b]1.0 kg/m^3 = 3.613 x 10^{-5} lb/in^3.
[c]ACI 318–14 (2014) code.
[d]Typical lower bound Asphalt concrete properties at 21 °C (70 °F).
[e]Typical lower bound properties for well compacted subgrade.
[f]The existing culvert is in good structural condition (no cracks or spalling). A resilient modulus less than 138 MPa (20,000 psi) will cause structural failure in an elastic FE analysis.
[g]Typical lower bound properties for well compacted crushed stone base.

are the axle loads of the legal trucks considered for rating analysis. For the current 2-D model, which furnished a discrete FE model for the soil surrounding the arch culvert, the software automatically computed dead loads as long as proper material densities were given. Nine trucks, routinely considered for load rating bridges in the state of Kentucky, were used in the FE analysis as live loads. These included the AASHTO HS-20 truck, Kentucky legal trucks (KY1, KY2, KY3, and KY4), and AASHTO special hauling vehicles (SHV No. 4, 5, 6, and 7).

Supplementary material Table A1 summarizes the truck configurations and weights. The truck wheel load, which is assumed to be a concentrated force placed at the center of tire contact area, and applied at the pavement level, dissipates through the soil in two directions, longitudinally (or parallel to the culvert's cross section) and transversely (or perpendicular to culvert's section) (Lawson et al., 2017; Wood et al., 2016). This implies that as the culvert fill height increases, the effects of live load become smaller (Acharya, 2012). In the 2-D FE model, the truck load dissipates naturally in the longitudinal direction through the soil elements without the need to use any distribution equations (Lawson et al., 2017). However, transverse live load dissipation cannot be considered in two-dimensional models, a limitation for this model class, but can be indirectly included using theoretical distribution formulas that calculate the effective width (E) through which the load

Table 2. Geometrical properties of RC arch culverts.

Culvert ID	Span m (ft.)	Rise m (ft.)	Span/rise	Fill m (ft.)
B-55N	9.14 (30.00)	5.48 (18.00)	1.67	10.67 (35.00)
B-32N	9.45 (31.00)	4.75 (15.60)	2.00	2.44 (08.00)
B-41N	9.75 (32.00)	6.00 (20.00)	1.00	2.44 (08.00)
B-20 N	10.36 (34.00)	4.42 (14.50)	2.34	7.62 (25.00)
B-94N	7.92 (26.00)	5.03 (16.50)	1.56	14.78 (48.50)
B-3N	10.36 (34.00)	4.42 (14.50)	2.34	6.09 (20.00)
B-10N	6.70 (22.00)	3.39 (14.40)	1.53	6.09 (20.00)
B-62N	6.40 (21.00)	6.34 (20.80)	1.00	7.62 (25.00)
B-32N	6.70 (22.00)	5.03 (16.50)	1.33	12.19 (40.00)
B-97N	10.36 (34.00)	4.42 (14.50)	2.34	7.62 (25.00)
B-50N	14.50 (47.50)	8.65 (28.38)	1.67	12.19 (40.00)
B-1N	7.62 (25.00)	6.55 (21.50)	1.16	7.01 (23.00)
B-4 N	9.60 (31.50)	6.40 (21.00)	1.50	9.14 (30.00)
B-35N	12.19 (40.00)	5.98 (19.63)	2.00	6.09 (20.00)
B-27N	10.36 (34.00)	6.25 (20.50)	1.66	6.09 (20.00)
B-26N	10.97 (36.00)	5.33 (17.50)	2.00	6.09 (20.00)
B-35L	6.70 (22.00)	4.42 (14.50)	1.52	18.29 (60.00)
B-20N	10.36 (34.00)	6.22 (20.42)	1.67	3.05 (10.00)
5B-66N	6.70 (22.00)	4.42 (14.50)	1.52	3.05 (10.00)
5B-70L	9.75 (32.00)	4.72 (15.50)	2.00	4.57 (15.00)
B-23N	8.38 (27.25)	4.09 (13.42)	2.00	6.09 (20.00)

dissipates. The AASHTO LRFD Bridge Design Specifications for Highway Bridges (AASHTO, 2017) is used herein to determine E for one line of wheel loads and fill depths less than 2 ft:

$$E\ (\text{ft.}) = 4 + 0.06 \times S \leq 7\ \text{ft.} \tag{2}$$

where S is the culvert's span length in ft.

Given the culvert spans available in this study (Table 2), which ranged between 6.40 and 14.50 m (21 and 47.5 ft.), values for E were between 1.60 and 2.13 m (5.25 and 7 ft.). Due to the small variation in E values, and to provide a unified truck load inputs for the FE model for all culverts, E was assumed to be the typical truck wheel spacing of 1.8 m (6 ft.). For culverts, when the fill depth is more than 0.61 m (2 ft), AASHTO recommends that the concentrated wheel load be uniformly distributed over a square with sides equal to 1.75 times the fill height. Therefore, taking E as 1.83 m (6 ft) is conservative for the fill heights of the culverts shown in Table 2. The truck wheel load is then divided by E to generate a transversely-dissipated live load for input in the FE model. Within the FE model, each truck wheel load was placed initially on the left-upper corner of the model, at the pavement level. Trucks were them moved across the entire length of the model in movement steps of 0.30 m (1 ft.).

5. Evaluation of the FE model

A comparative study was carried out to validate the proposed 2-D FE model and its assumptions in predicting the RC arch forces needed for the load rating procedure. A full-scale RC arch culvert tested by McGrath and Mastroianni (2002) was used to validate the FE model. The culvert had a span of 8.5 m (28 ft.), rise of 2 m (6.5 ft.), wall thickness of 228.6 mm (9 in.), and fill height (above the arch) of 0.3 m (1 ft.). Although validating the results against a culvert with a larger fill height would have provided more confidence in the model, as well as meeting the objective and focus of this study, the in-situ test presented by McGrath and Mastroianni (2002) was the only field test known to the authors to focus on RC arch culverts. The culvert was subjected to an incremental simulated single-axle live load (P) located above the arch's crown. The FE geometric model was generated following the assumptions outlined in the previous sections, while material properties were those given by McGrath and Mastroianni (2002).

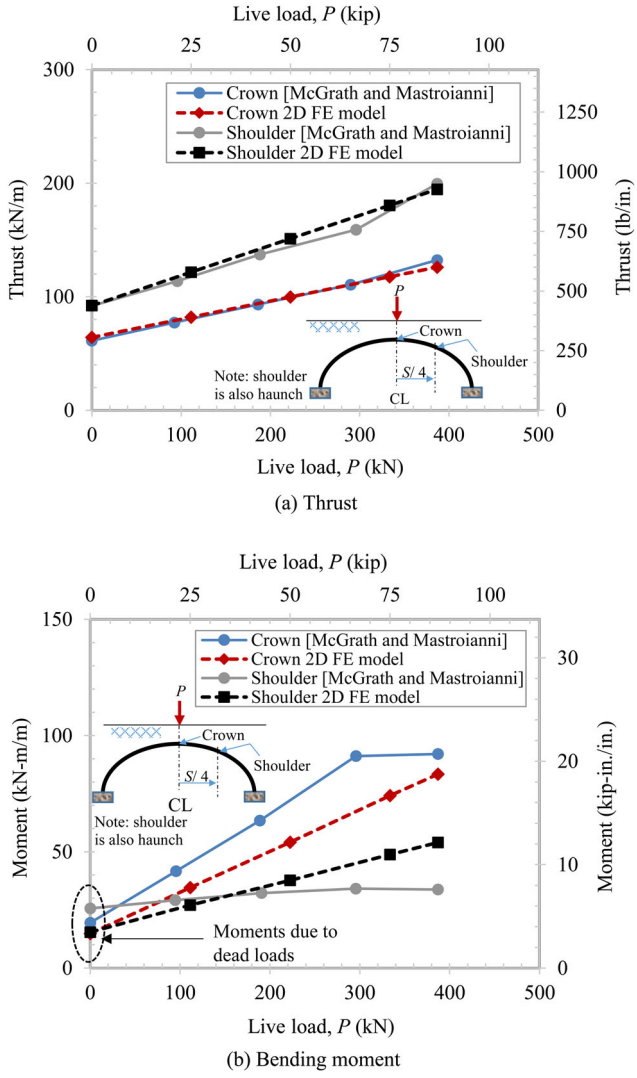

Figure 5. Comparisons between current 2 D FE model and McGrath and Mastroinni test.

Figure 5 compares the FE model predictions and results from field testing [McGrath and Mastroianni (2002)] for the thrust and bending moment at the crown and shoulder as a point load (P), applied on the roadway over the crown, is increased from 0 to 387 kN. The thrust comparison in Figure 5(a) shows very good agreement between the experimental and 2 D FE results. The maximum difference was less than 3% (when $P = 387$ kN) at the crown and less than 10% (when $P = 300$ kN) at the shoulder. In Figure 5(b), the difference between the experimental and 2 D FE results for bending moment is more pronounced with a maximum difference reaching 50%.

The experimental and 2 D FE crown deflections, Δ_c, are compared in Figure 6 for different magnitudes of point

loads, P, applied on the roadway over the crown. The FE P-Δ_c relationship is linear elastic due to linear elastic material properties adopted in the FE model. The FE and experimental deflections compare very up to deflections below 17 mm at a load nearing $P = 1000$ kN. When $\Delta c > 17$ mm, the two deflections diverge as the effect of the soil nonlinearity increase with P for values of $P > 500$ kN.

The difference between FE and experimental results for thrust, moments, and deflections can be attributed to a number of factors, including: (a) difference between reported and actual material and geometric properties used in testing, (b) approximations used experimentally to convert strain measurements to moments and thrusts, (c) FE model assumptions and simplifications(e.g. boundary conditions, 2 D modeling, material properties). Similar differences have been observed between 2 D FE models for box culverts, which were adopted in load rating guides (Acharya, 2012; Wood et al., 2016), and experimental results. Wood et al. (2015) reported that predicted-to-tested live-load moments for box culverts, with a fill height of 0.5 m (1.5 ft.), ranged from 0.4 to 46.7, with an inner quartile of 3.5.

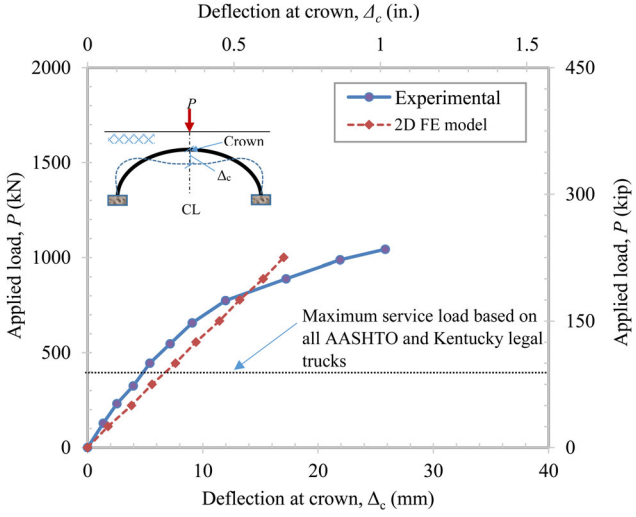

Figure 6. Load vs. crown deflection (P-Δ_c) comparisons between experimental results (McGrath & Mastroianni, 2002) and 2 D FE model.

6. Load rating procedure

The load rating of RC arch culverts was carried out in accordance with the guidance of the MBE (2015). The load rating analysis was performed for two rating methods, LFR and ASR. For both rating methods the inventory level and operating level ratings were also considered. The rating factor (RF) was found using [(MBE 2015)]:

$$RF = \frac{C - A_1 D}{A_2 L(1 + I)} \tag{3}$$

where:

RF = Rating factor for the live-load carrying capacity;

C = Capacity of member (bending, shear, axial, torsion, etc.);

D = Dead load effect on member (bending, shear, axial, torsion, etc.);

L = Live load effect on member (bending, shear, axial, torsion, etc.);

Table 3. Results of 2-D FE models of RC arch culverts.

	Moment at crown			Moment at haunch[a]			Thrust at springing		
Culvert ID	M_D[b] (kN-m)[c]	M_L[d] (kN-m)	%[e]	M_D[b] (kN-m)	M_L[d] (kN-m)	%[e]	F_D[f] (kN)[g]	F_L[h] (kN)	%[e]
B-55N	27.23	1.3	4.78	65.42	2.32	3.55	542.66	7.92	1.46
B-32N	5.09	0.91	17.88	14.81	1.36	9.19	177.92	12.45	7.00
B-41N	8.59	0.97	11.30	13.90	1.30	9.36	213.51	12.45	5.84
B-20 N	8.93	0.68	7.62	27.46	1.33	4.85	382.53	11.12	2.91
B-94N	25.20	0.8	3.18	56.49	1.25	2.22	604.93	7.11	1.18
B-3N	7.69	0.68	8.85	23.73	1.25	5.27	105.42	11.56	3.43
B-10N	6.33	0.46	7.27	16.84	1.02	6.06	338.05	10.23	3.84
B-62N	4.98	0.42	8.44	6.78	0.40	5.90	266.88	6.67	3.04
B-32N	25.20	0.97	3.85	47.23	1.36	2.88	220.18	7.12	1.53
B-97N	8.93	0.68	7.62	34.12	1.53	4.49	467.04	9.34	2.53
B-50N	37.06	0.8	2.16	108.58	1.93	1.78	369.63	9.78	2.65
B-1N	23.28	1.25	5.37	39.43	1.59	4.04	370.08	8.90	2.36
B-4N	42.03	1.7	4.05	52.99	1.81	3.42	200.16	8.90	1.79
B-35N	20.34	1.36	6.69	60.00	2.49	4.15	378.08	11.12	2.74
B-27N	11.98	0.8	6.68	38.76	1.70	4.39	498.18	10.23	2.83
B-26N	11.64	0.91	7.82	36.95	1.70	4.61	406.11	10.67	3.05
B-35L	26.89	0.46	1.72	45.65	0.63	1.39	361.63	4.45	0.77
B-20N	8.59	0.76	8.85	24.41	1.36	5.58	350.95	13.79	5.94
B-66N	8.93	1.25	14.00	14.92	1.93	12.94	578.24	5.78	6.99
B-70L	9.16	0.97	10.59	22.83	1.47	6.44	578.24	11.12	4.58
B-23N	5.88	0.51	8.68	14.13	0.97	6.87	232.19	8.45	3.60

[a]Haunch refers to the quarter-span point.
[b]Bending moment due to dead loads (self-weight of the RC arch, footing, soil parts, and pavement)
[c]1.0 kN-m = 8850 lb-in.
[d]Bending moment due to effects of HS-20 truck
[e]Percentage of live load action (e.g. M_L, F_L) to the dead load action (e.g. M_D, F_D)
[f]Axial force (thrust) at springing point due to dead loads (self-weight of RC arch, , footing, soil parts, and pavement)
[g]1.0 kN= 224.8 lb.
[h]Axial force (thrust) at springing point due to effects of HS-20 truck

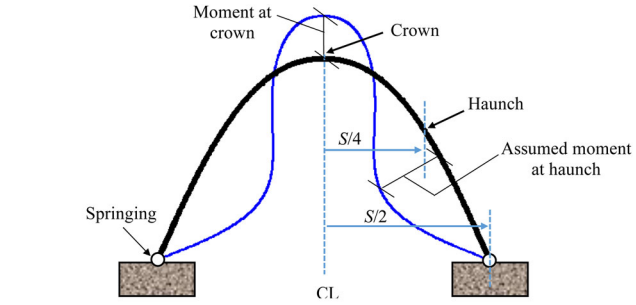

(a) Bending moment.

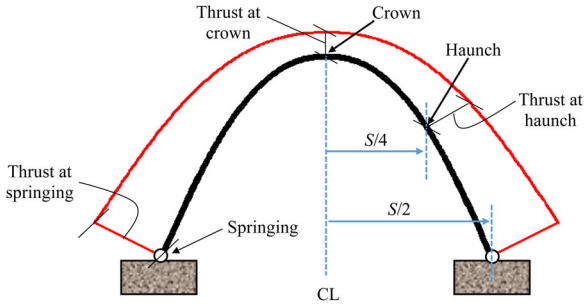

(b) Axial force (thrust).

Figure 7. Typical bending moment and thrust diagrams in RC arch culverts.

I = Impact factor to be used with the live load effect, determined according to the specifications of AASHTO (2002), section 3.8.2;

A_1 = Factor for dead loads, =1 (for ASR method), and =1.3 (for LFR method);

A_2 = Factor for live loads, =1 (for ASR method), = 2.17 (for LFR method, Inventory level), and = 1.30 (for LFR method, Operating level).

After determining the rating factor, *RF* was multiplied by the rating vehicle in kN/tons to give the rating of the RC arch culvert:

$$RT = (RF) \times W \tag{4}$$

where:

RT = culvert rating in tons;

W = weight (kN/tons) of nominal truck used in determining the live load effect.

RC arch structures are generally rated for axial forces and bending moment, since multiple studies found that these actions are more critical when compared with forces such as shear (Chajes, 2002; Kim et al., 2009). The interaction between bending moment and axial force was neglected. Although load rating analysis can be performed for any number of points along the arch, fewer points are preferred in order to execute a simple rating procedure. Due to the effects of large fill heights (the culverts in this study had fill ranges between 2.4 to 18.3 m [8 to 60 ft.]), bending moments and thrusts resulting from dead loads were much larger than similar forces exerted by live loads. Table 3 lists the moments at crown and haunch and thrusts at springing due to dead loads and HS-20 live load. The table shows that the ratio of live load to dead load moments ranged from 1.72 to 17.88 for crown, and 1.39 to 12.94 for haunch. The ratio of live load to dead load thrust at springing was between 0.77 and 7.00. Similar results were observed for other trucks used in the study.

Table 4. Inventory load rating factors, for HS-20 truck.

		ASR method		LFR method	
Culvert ID	Fill m (ft.)	$RF^{a,b}$	Critical section	$RF^{a,b}$	Critical section
B-32N	2.44 (08.00)	5.30	Crown	3.57	Crown
B-41N	2.44 (08.00)	4.10	Crown	5.22	Crown
B-20 N	7.62 (25.00)	3.89	Haunch	3.20	Haunch
B-3N	6.09 (20.00)	4.09	Haunch	3.28	Haunch
B-10N	6.09 (20.00)	0.18	Crown	0.60	Crown
B-62N	7.62 (25.00)	3.72	Haunch	2.89	Haunch
B-35N	6.09 (20.00)	11.16	Crown	19.77	Crown
B-27N	6.09 (20.00)	0.72	Crown	1.43	Crown
B-26N	6.09 (20.00)	1.65	Haunch	1.75	Haunch
B-20N	3.05 (10.00)	1.87	Crown	1.60	Crown
B-66N	3.05 (10.00)	4.50	Crown	3.09	Crown
B-70L	4.57 (15.00)	6.74	Crown	4.57	Crown
B-23N	6.09 (20.00)	0.38	Haunch	0.72	Haunch

[a]Minimum rating factor obtained from rating analysis for all applicable actions (bending moments, and axial forces) and at corresponding critical points (springing, haunch, and crown).
[b]Controlling *RF* is always bending moment.

While the FE model provided the capacity to evaluate the load rating at numerous locations, to preserve the load rating analysis's simplicity, the locations were chosen based on the appearance of axial and bending moment diagrams from dead loads alone. Figure 7 displays characteristic bending and thrust diagrams of a typical RC arch culvert subjected to dead loads. Based on the composition of these diagrams, the following points were selected to perform load rating analysis of RC arch culverts having large fills: (1) crown and haunch for bending moment effects, and (2) crown, haunch, and springing for thrust effects. After selecting the points for the load rating procedure, the FE model was used to determine the dead load (D) and live load effects (L) at each of the above points (see Equation (3)). The section capacity (C) at the respective point(s) was derived from fundamental concrete design procedures and guidance of the MBE (2015).

7. Results and discussion

Equation (3), along with the FE models (which calculated dead and live load effects) and capacities determined from design procedures, were used to calculate rating factors (*RFs*). For individual trucks, *RFs* were found for the bending and axial actions at the critical points mentioned previously. The minimum *RF* of all points was selected as the rating factor of the entire arch culvert. Notably, in all 21 culverts and for all trucks, *RFs* for thrusts were always larger than *RFs* for bending moments. This indicates that the bending moment controls the rating. Table 4 lists the inventory *RFs* for the HS-20 truck, using ASR and LFR methods, for several culverts. When the fill is small [2.4 to 6.1 m (8 to 20 ft.)], the critical section (where the minimum *RF* occurs) is located at the crown. For larger fills, the critical section

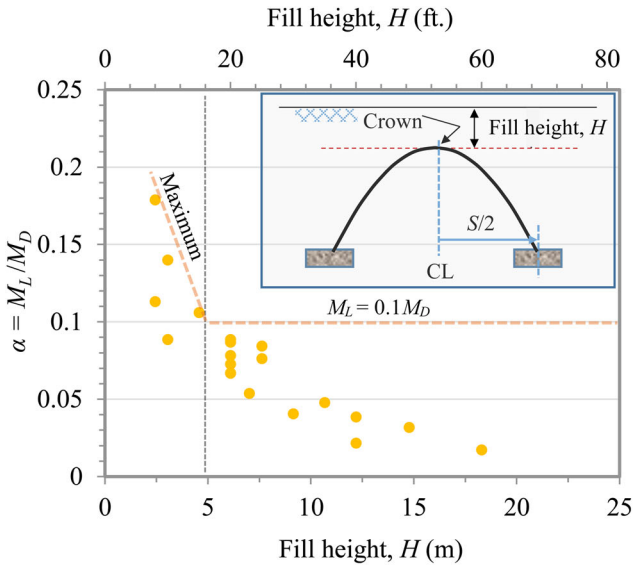

(a) Bending moments at crown.

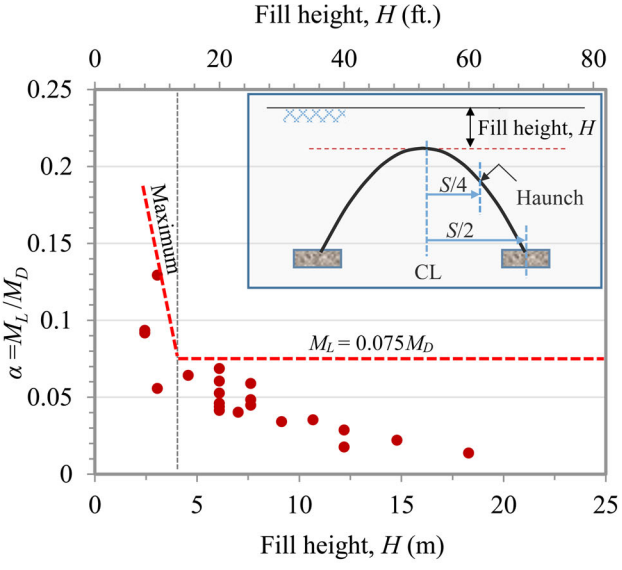

(b) Bending moments at haunch.

Figure 8. Variation in the live load moment to dead load moment ratio ($\alpha = M_L/M_D$) vs. fill height (H) for RC culverts.

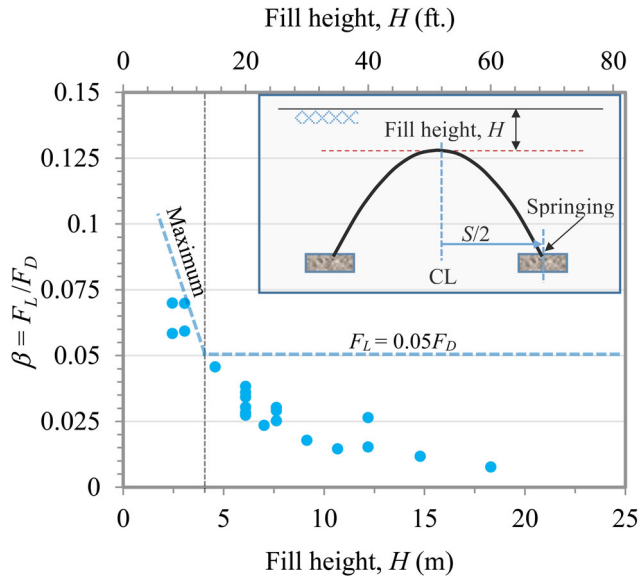

Figure 9. Variation in the live load thrust to dead load thrust ratio ($\beta = F_L/F_D$) vs. fill height (H) for RC culverts.

shifts to the haunch. This trend was also observed in all other trucks.

The current rating procedure, followed in MBE (2015), does not address arch culverts with large fills in which the effects of live loads diminish as the culvert's fill increases. To illustrate this numerically, the denominator of Equation (3) becomes negligible when the culvert fill increases due to the dissipation of the live load through the soil. Figures 8 and 9 show this trend for the arch culverts examined in this study, where Figure 8 presents the ratio of live load moment (M_L) to dead load moment (M_D) at the crown and haunch and Figure 9 plots the ratio of live load thrust (F_L) to dead load thrust (F_D) at springing, with respect to the culvert fill, obtained from the FE models. Live load effects diminish as culvert fill increases. AASHTO specifications (AASHTO, 2002) recognize this situation and permits neglecting live load effects for culverts with fill heights that are the larger of 2.4 m (8 ft.), the span length for single-span culverts, or the distance between faces of outer walls for multiple-span culverts. Experimental research by Abdel-Karim, Tadros, and Benak (1990) also noticed that live load pressures become exceedingly small for fill depths greater than 2.4 m (8 ft) for tested box culverts, and suggested live load effects be ignored when it contributes less than 5% of the total load effects.

To avoid the mathematical error of having close-to-zero denominator in Equation (3), which leads to an incorrectly large or infinite *RF* value, the rating formula must be readjusted for culverts with large fill heights. First, the threshold for deep culverts needs to be set. For RC arch culverts with geometrical properties similar to the culverts considered in this study, which have a single span, a general parabolic arch shape, and a span/rise ratio of 1 to 2.34, the threshold is defined based on results of Figures 8 and 9. The live load effects are less than 10% for (M_L/M_D) at both the crown and haunch, and (F_L/F_D) at springing is less than 5%, when the accompanying fill [also considered as the threshold for deep culverts] is approximately 4.9 m (16 ft.) or more.

Based on our results, we propose adjusting the rating procedure for RC arch culverts with fills larger than 4.9 m (16 ft.). In the proposed method, *RF* is given by:

$$RF = \frac{C - A_1 D}{0.1D}, \text{ for fills } \geq 4.9 \text{ m } (16\text{ft.}) \qquad (5)$$

As previously stated, the thrust (Figure 9) does not govern for fill heights greater than 2.4 m (8 ft.). The proposed modified rating equation (Equation (5)) is based on the FEA results for the bending moments in Figure 8. The higher limit of 0.1 D, instead of 0.05 D (Abdel-Karim et al., 1990), for fill heights greater than 4.9 m (16 ft.), was chosen to provide conservative load ratings. It should be noted that the

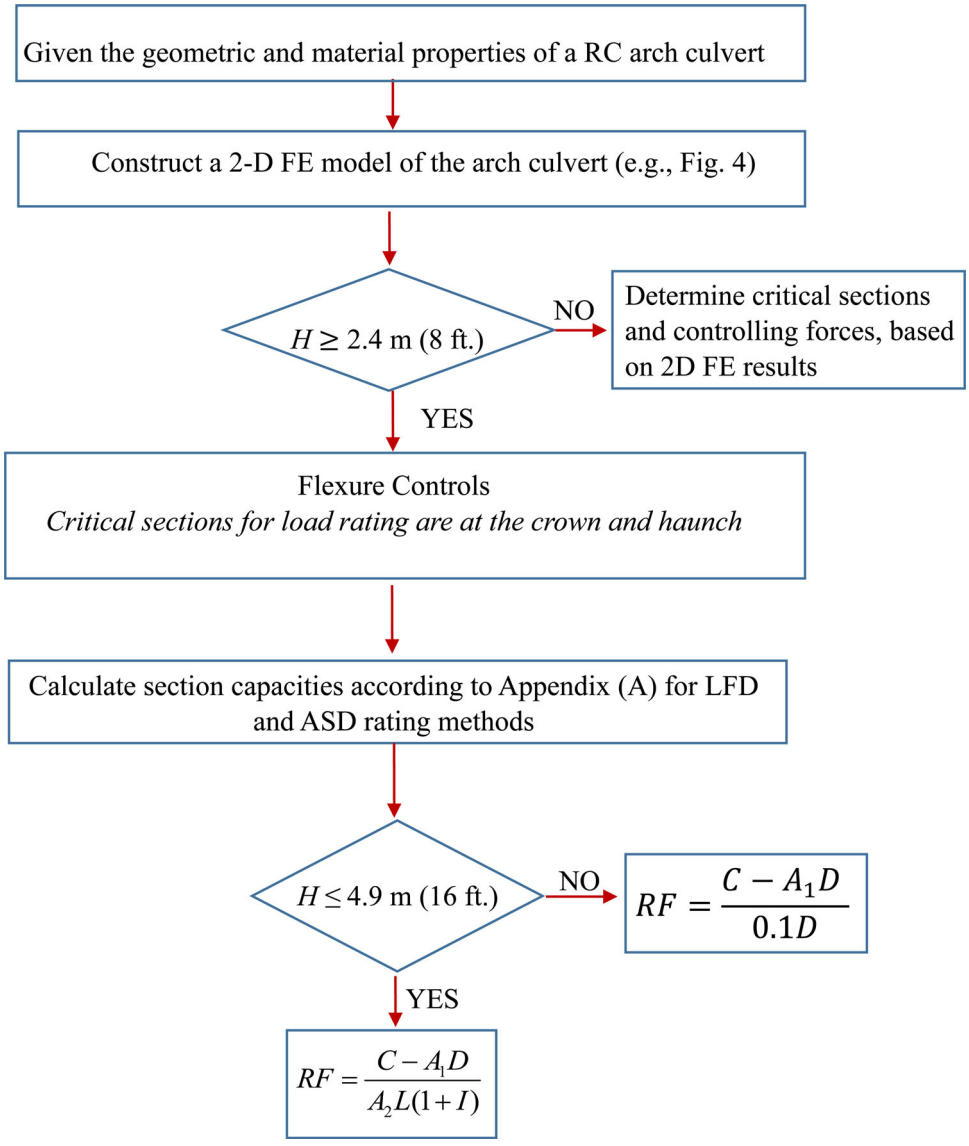

Figure 10. Steps for load rating simply supported, single-span, parabolic RC arch culverts with 1.3 ≤ Span/Rise ≤ 2.3.

proposed fill height is more than double the height that Abdel-Karim et al. (1990) found the live load effects to be negligible. The flowchart in Figure 10 summarizes the rating methodology and basic steps to follow when load rating RC arch culverts that have geometrical and mechanical characteristics similar to the culverts analyzed in this study.

Figure 11 presents the operating-level rating factors (*RF*s) for seven of the culverts whose *RF*s were less than 10 for the nine trucks considered in this study (Table A1). It should be noted that since the objective is to evaluate the trends based in the truck types, Equation (5) was not utilized when calculating the *RF*s in Figure 11. When comparing the standard AASHTO HS20 truck with the Kentucky legal trucks, Figure 11(a) shows that the KY3 and KY4 had the lowest RFs for five of the seven culverts. This is likely because of their larger gross vehicle weight (W) and heavy, closely spaced rear axles (Table A1). Similarly, Figure 11(b) shows that the *RF*s for the special hauling vehicle and SU7 were less than the *RF*s for the HS 20 for all seven culverts, while the SU4 truck had the lowest ratings. The results presented in Figure 11 support the findings presented by Sivakumar et al. (2007) and emphasize the need to include the rating for the special hauling vehicles in load rating practices and guidelines.

8. Conclusions

This study investigated the load rating of bridge-size RC arch culverts. It proposes an alternative analysis method that overcomes the limitations of the widely followed elastic frame concept. The method uses 2-D FE models that automatically and accurately calculate gravity loads for all parts and includes the soil's passive pressure as result of discrete modeling of soil media in the vicinity of the arch. Furthermore, the proposed FE models include a method to accurately represent truck loads on the culverts. This is achieved by generating the entire truck (with respective axle weights and spaces) and moving it across the length of the

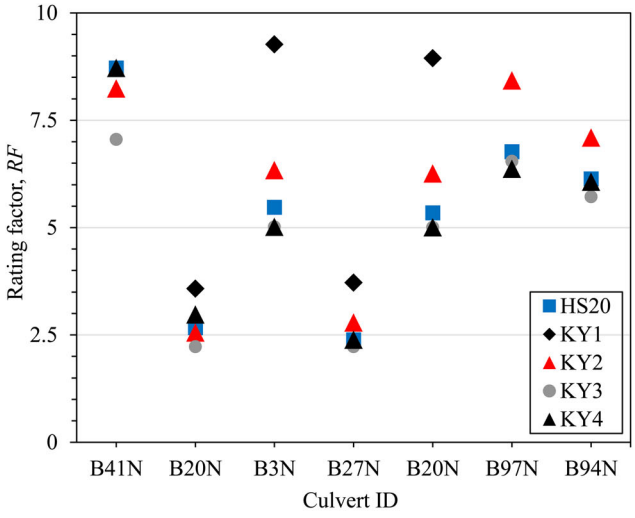

(a) HS20 and Kentucky type trucks

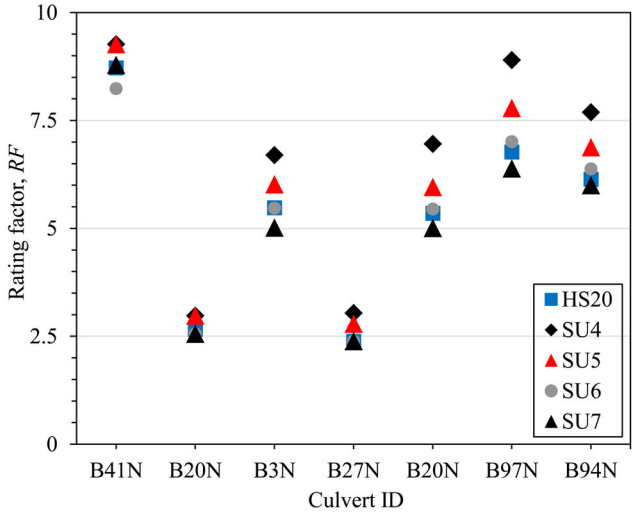

(b) HS20 and SHV type trucks

Figure 11. Operating-level rating factors for seven culverts and nine truck types.

model to determine maximum forces within the arch culvert. Several types of trucks (e.g. single, tandem, or multiple axles) can be input into the model. It can also handle the presence of several trucks.

The FE models were verified by comparing their outcomes with experimental tests on a full-scale RC culvert. The models were used to load rate 21 RC culverts with fill heights ranging from 2.4 m (8 ft.) to 18.3 m (60 ft.). Based on this study the following conclusions can be derived:

1. The proposed 2-D FEA method provides a more robust method for load rating RC arch culverts compared to the elastic frame method.
2. For culverts with fills larger than 2.4 m (8 ft.), the culvert rating can be obtained from calculations at few points – the crown and haunch points for bending moment effects, and the crown, haunch, and springing for thrust effects.
3. For culverts with fills larger than 4.9 m (16 ft.), live load effects are less than 10% of dead load effects.
4. For culverts with fills larger than 4.9 m (16 ft.), a modified load rating equation is proposed to avoid having extremely large rating results due to the small values for the live load effects.
5. The results presented in this study show that rating factors for Kentucky trucks KY2 and KY4 and special hauling vehicle type SU4 were governing in comparison to rating factors derived from the standard AASHTO HS20 truck.

Data availability statement

Some or all data, models, or code that support the findings of this study are available from the corresponding author upon reasonable request.

Disclosure statement

No potential conflict of interest was reported by the authors.

Funding

Funding for the project was provided by the Federal Highway Administration (FHWA) and the Kentucky Transportation Cabinet (KYTC).

References

Aagard, A. D. (2007). *Rectification of 2-D to 3-D finite element analysis in buried concrete arches under discrete loading* (master's thesis). Department of Civil and environmental engineering, Brigham Young University, Provo, UT.

Abdel-Karim, A. M., Tadros, M. K., & Benak, J. V. (1990). Live load distribution on concrete box culverts. *Transportation Research Record (TRR): Journal of the Transportation Research Board, 1288*, 136–151.

Acharya, R. (2012). *Improved load distribution for load rating of low-fill box structures* (master's thesis). Lawrence, Kansas: University of Kansas. Retrieved from https://kuscholarworks.ku.edu/handle/1808/10630

ACI 318-14. (2014). *Building code requirements for reinforced concrete* (ISO# 193382007E). Farmington Hills, Michigan: American Concrete Institute.

American Association of State Highway and Transportation Officials. (2002). *AASHTO standard specifications for highway Bridges* (17th ed.). Washington, D.C.: AASHTO.

American Association of State Highway and Transportation Officials. (2015). *Manual for bridge evaluation (2nd Edition) with 2015 Interim Revisions.* Washington, DC: AASHTO.

American Association of State Highway and Transportation Officials. (2017). *AASHTO LRFD bridge design specifications* (7th ed.). Washington, DC: AASHTO.

Andersson, A. (2011). *Capacity assessment of arch bridges with backfill, Case of the old Årsta railway bridge* (PhD thesis), Bulletin 107. KTH Royal Institute of Technology, Sweden.

Bjurstrom, H., & Lasell, J. (2009). *Capacity assessment of a single span arch bridge with backfill - A case study of the Glomman Bridge* (master's thesis). KTH Royal Institute of Technology, Sweden.

Boothby, T. E., Domalik, D. E., & Elgin, C. S. (1997). Load rating of masonry arch bridges and culverts (Res. Rep. No. FHWA/OH-96/016, Nat. Tech. Infor. Service No. PB-97-1485555). Columbus, OH: Ohio Department of Transportation.

Boothby, T. E., & Fanning, P. J. (2002). *Assessment methods for masonry arch bridges*. Proceedings of Structural Faults and Repair Conference (6 p.).

Boothby, T. E., & Fanning, P. J. (2004). Load-rating of masonry arch bridges: Refinements. *Journal of Bridge Engineering, ASCE*, *9*(3), 304–307. doi:10.1061/(ASCE)1084-0702(2004)9:3(304)

Boothby, T. E., Fanning, P. J., & Roberts, B. J. (2000). Modeling, assessment, and load-rating of masonry arch bridges. Transportation Research Board 79th Annual Meeting (Paper No. 000394.6).

Brencich, A., & Francesco, U. D. (2004). Assessment of multispan masonry arch bridges. I: Simplified approach. *Journal of Bridge Engineering*, *9*(6), 582–590. doi:10.1061/(ASCE)1084-0702(2004)9:6(582)

Chajes, M. (2002). Load rating of arch bridges (Technical Report). Newark, DE: Delaware Center for Transportation, University of Delaware.

Citto, C., & Woodham, D. (2014). Evaluation and rating of masonry arch bridges. *Proceedings of the 2014 Structures Congress: April 3-5, 2014*, Boston, MA.

Department of Transport, UK. (1993). The assessment of highway bridges and structures (A 16/93). London, UK: Her Majesty's Stationary Office.

Fanning, P. J., & Boothby, T. E. (2002). Three-dimensional modeling and full-scale testing of stone arch bridges. *Computers & Structures*, *79*, 2645–2662.

Fanning, P. J., Boothby, T. E., & Roberts, B. J. (2001). Longitudinal and transverse effects in masonry arch assessment. *Construction and Building Materials*, *15*(1), 51–60. doi:10.1016/S0950-0618(00)00069-6

Federal Highway Administration. (2012). Bridge inspector's reference manual (FHWA Report NHI 12-049, 2,004 pp.). Washington, DC.

Gilbert, M., Melbourne, C., & Smith, C. (2006). Discussion of "assessment of multispan masonry arch bridges. I: Simplified approach" by Brencich and Francesco. *Journal of Bridge Engineering, ASCE*, *11*(2), 257–261. doi:10.1061/(ASCE)1084-0702(2006)11:2(257)

Halden, D. (1995). *Performance criteria in arch bridge assessment*. Arch Bridges: Proceedings of the First International Conference on Arch Bridges (pp. 439–448), Bolton, UK Thomas Telford, London.

Hopkins, T. C., Beckham, T. L., Sun, C., & Ni, B. (2001). Resilient modulus of Kentucky soils (Technical report No. KTC-01-07/SPR-163-95-1F). Lexington, KY: Kentucky Transportation Center, University of Kentucky.

Katona, M. G., Meinhert, D. F., Orillac, R., & Lee, C. H. (1979). Structural evaluation of new concepts for long-span culverts and culvert installations (Report No. FHWA-RD-79-115). Washington, DC: Federal Highway Administration.

Kim, J. S., Garro, R., & Doty, D. (2009). A simplified load rating method for masonry and reinforced concrete arch bridges. *Proceedings of AREMA Annual Conference 2009* (37 p.).

Krajcinovic, D. (1996). *Damage mechanics*. New York: Elsevier.

Lawson, W., Seo, H., Surles, J., & Morse, S. (2018). Impact of specialized hauling vehicles on load-rating older, bridge-class, reinforced concrete box culverts. *Transportation Research Record: Journal of the Transportation Research Board*, *2672*(41), 87–14. doi:10.1177/0361198118781148

Lawson, W. D., Seo, H., Surles, J. G., & Morse, S. M. (2017). *Culvert rating guide* (2nd ed.). Austin, TX: Texas Department of Transportation.

Lekhnitskii, S. G. (1963). *Theory of elasticity of an anisotropic elastic body*. P. Fern (Trans.). San Francisco: Holden Day.

Massachusetts Department of Transportation. (2013). *LRFD bridge manual-2013 edition*. Boston, MA.

McGrath, T. J., & Mastroianni, E. P. (2002). Finite-element modeling of reinforced concrete arch under live load. *Transportation Research Record: Journal of the Transportation Research Board*, *1814*(1), 203–210. doi:10.3141/1814-24

Mousavi, S. M., Jayawickrama, P. W., Wood, T. A., & Lawson, W. D. (2017, March 12–15). *Selection of soil stiffnesses for the load rating of in-service culverts*. Geotechnical Frontiers 2017 Transportation Facilities, Structure, and Site Investigation GSP 277, Orlando, FL. doi:10.1061/9780784480441.024

Seo, H., Wood, T. A., Javid, A. H., & Lawson, W. D. (2017). Simplified, system-level pavement stiffness model for box culvert load rating applications. *Journal of Bridge Engineering*, *22*(10), 04017066. doi:10.1061/(ASCE)BE.1943-5592.0001098

Sivakumar, B., Moses, F., & Ghosn, M. (2007). Legal truck loads and AASHTO legal loads for posting (Report 575, Project 12–63). Washington, DC: The National Cooperative Highway Research Council, Transportation Research Board.

STAAD Pro V8i. (2012). *Technical reference manual*. Exton, PA: Bentley Structures, Inc.

Wood, T. A., Lawson, W. D., Jayawickrama, P. W., & Newhouse, C. D. (2015). Evaluation of production models for load rating reinforced concrete box culverts. *Journal of Bridge Engineering*, *20*(1), 04014057. doi:10.1061/(ASCE)BE.1943-5592.0000638

Wood, T. A., Lawson, W. D., Surles, J. G., Jayawickrama, P. W., & Seo, H. (2016). Improved load rating of reinforced concrete box culverts using depth-calibrated live load attenuation. *Journal of Bridge Engineering*, *21*(12), 04016095. doi:10.1061/(ASCE)BE.1943-5592.0000967

Wood, T., Surles, J., Mousavi, M. S., Jayawickrama, P., Javid, A. H., Seo, H. Y., & Lawson, W. (2017, March 12–15). Modeling factors influencing culvert load rating: a parametric analysis. Paper #170030, Geotechnical Special Publication No. 277: Transportation Facilities, Structures, and Site Investigation (pp. 243–252), ASCE Geotechnical Frontiers, Orlando, FL.

Wu, X. (2010). Load rating of existing masonry arch bridges in USA. *6th International Conference on Arch Bridges*, Fuzhou, China.